[14] Goodman, L. E. and Sutherland, J. G., "Natural Frequencies of Continuous Beams of Uniform Span Length," *Journal of Applied Mechanics*, Vol. 18, No. 2, June 1951, pp. 217–218.
[15] Huang, T. C., "The Effect of Rotatory Inertia and of Shear Deformation on the Frequency and Normal Mode Equations of Uniform Beams with Simple End Conditions," *Journal of Applied Mechanics*, Vol. 28, No. 4, Dec. 1961, pp. 579–584.
[16] Hurty, W. C. and Rubinstein, M. F., *Dynamics of Structures*, Prentice-Hall, Englewood Cliffs, N.J., 1964.
[17] Lee, P. C. Y. and Nikodem, Z., "An Approximate Theory for High-Frequency Vibrations of Elastic Plates," *International Journal of Solids and Structures*, Vol. 8, No. 5, 1972, pp. 581–612.
[18] Kruszewski, E. T., "Effect of Transverse Shear and Rotatory Inertia on the Natural Frequency of a Uniform Beam," TN 1909, May 1949, NACA.
[19] Leonard, R. W. and Budiansky, B., "On the Traveling Waves in Beams," TN 2874, Jan. 1953, NACA.
[20] Mindlin, R. D., "Influence of Rotatory Inertia and Shear on Flexural Motions of Isotropic, Elastic Plates," *Journal of Applied Mechanics*, Vol. 18, No. 1, March 1951, pp. 31–38.
[21] Mindlin, R. D. and Deresiewiez, H., "Timoshenko's Shear Coefficient for Flexural Vibrations of Beams," TR 10, ONR Project, NR064-388, 1953, Dept. of Civil Engineering, Columbia University, New York.
[22] Nelson, R. B., Dong, S. B., and Kalra, R. D., "Vibrations and Waves in Laminated Orthotropic Circular Cylinders," *Journal of Sound and Vibration*, Vol. 18, No. 3, 1971, pp. 429–444.
[23] Roark, R. J., *Formulas for Stress and Strain*, 3rd ed., McGraw-Hill, New York, 1954, pp. 119–121.
[24] Timoshenko, S., "On the Corrections for Shear of the Differential Equation for Transverse Vibrations of Prismatic Bars," *Philosophical Magazine*, Vol. 41, May 1921, pp. 744–746.
[25] Timoshenko, S., "On the Transverse Vibrations of Bars of Uniform Cross-Sections," *Philosophical Magazine*, Vol. 43, 1922, pp. 125–131.

MAY 1974 AIAA JOURNAL VOL. 12, NO. 5

Nonlinear Panel Response by a Monte Carlo Approach

R. VAICAITIS*
Columbia University, New York, N.Y.

AND

E. H. DOWELL† AND C. S. VENTRES‡
Princeton University, Princeton, N.J.

The vibration of clamped and simply supported elastic panels due to subsonic and supersonic turbulent boundary-layer flows is investigated by a Monte Carlo technique. The resulting generalized random forces are simulated numerically from boundary-layer turbulence spectra and the response analysis is performed in time domain. The mutual interaction between panel motion and external and/or internal airflow is included. Response studies are performed with respect to rms response, probability structure, peak distribution, threshold crossing and spectral density. The effect on the response statistics of in-plane loading, static pressure differential and cavity pressure is investigated.

Nomenclature

a = plate length
a_∞ = velocity of sound, external flow
a_c = velocity of sound, cavity flow
b = plate width
b_{ij} = nondimensional modal amplitude
D = $Eh^3/12(1-\nu^2)$, plate stiffness
d = cavity depth
E = modulus of elasticity
$\mathbf{i}$ = imaginary unit $(-1)^{1/2}$
h = plate thickness
k_1, k_2 = wave numbers in x, y directions, respectively
M = Mach number, u_∞/a_∞
r, n = mode numbers
q = $\frac{1}{2}\rho_\infty u_\infty{}^2$, dynamic pressure
t = time
T = period
u_c = convection velocity
u_∞ = mean external flow velocity
w = plate deflections
x, y, z = spatial coordinates
ζ = boundary-layer displacement thickness
ζ^* = boundary-layer thickness
η = y/b
λ = $\rho_\infty u_\infty{}^2 a^3/2D$
λ^c = $\rho_c a_c{}^2 a^3/D$
μ = $\rho_\infty a/\rho_m h$
μ^c = $\rho_c a/\rho_m h$
ν = Poisson's ratio
ξ = x/a
ρ_m = plate material density/unit area
ρ_∞ = freestream density
ρ_c = cavity flow density
τ = $t(D/\rho_m h a^4)^{1/2}$
ω = frequency

Received August 14, 1973; revision received November 16, 1973. This work was supported by NASA Grant NGR 31-001-146.
Index categories: Structural Dynamic Analysis; Aeroelasticity and Hydroelasticity.

* Assistant Professor of Civil Engineering. Member AIAA.
† Professor, Department of Aerospace and Mechanical Sciences. Member AIAA.
‡ Research Staff, Department of Aerospace and Mechanical Sciences.

1. Introduction

IN Refs. 1–5, parametric studies were performed on nonlinear panel response and panel flutter using a time domain analysis. In Ref. 3 the boundary-layer turbulence was limited to gaussian white noise while in Ref. 5 the analysis considered only two streamwise modes. Simply supported boundary conditions were assumed in all of these cases. This paper is mainly concerned in studying statistical properties of nonlinear panel response to more realistic models of boundary layer turbulence and extending the analysis to clamped support boundary conditions.

A Monte Carlo technique is employed for the response analysis of panels undergoing large deformations under subsonic and

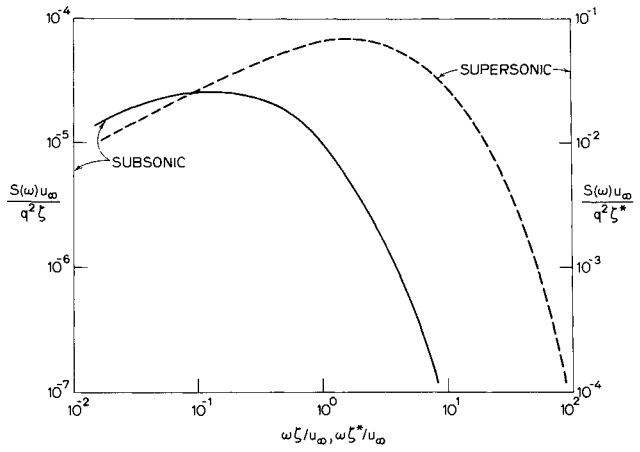

Fig. 1 Power spectra of boundary-layer turbulence.

supersonic turbulent boundary-layer pressure excitation. The mutual interaction between panel motion and external and/or internal airflow is included. The random pressure field from boundary-layer turbulence is taken as a stationary and homogeneous multidimensional gaussian random process having a mean value equal to zero. The random pressure is characterized by a power spectral density for which empirical expressions are presented in Ref. 6 for subsonic flow and in Ref. 7 for supersonic flow. Sketches of these spectra are shown in Fig. 1 while the empirical expressions are given in Sec. 3. Utilizing this information and simulation techniques of random processes[5,8,9] time and space histories of turbulent pressure are produced.

Response studies with respect to rms response, probability density function, peak distribution, threshold crossing and spectral density are performed. The effect of dynamic pressure, cavity pressure, in-plane loads, static pressure differential on panel response and response statistics is investigated for simply supported and clamped panels. Numerical examples are presented for subsonic and supersonic flow regions.

2. Panel Response

The deflection of an elastic panel immersed in a fluid flow and having geometric nonlinearity can be described by two nonlinear partial differential equations which are given in Refs. 1–3. In solving these nonlinear equations, plate deflection w is expanded in terms of orthogonal eigenfunctions corresponding to a linear plate model

$$w(x,y,t) = \sum_r \sum_n b_{rn}(t) X_r(x) X_n(y) \tag{1}$$

in which b_{rn} are response amplitudes and X_r are eigenfunctions which can be represented by $\sin(r\pi x/a)$ for a simple support boundary condition and by $\cos[(r-1)\pi x/a] - \cos[(r+1)\pi x/a]$ for a clamped plate. After the required stress functions are evaluated,[2,10] the assumed solutions are satisfied in Galerkin sense by computing integral average weighted in turn by each term of Eq. (1). The result is a system of simultaneous nonlinear integral-differential equations for $b_{mn}(t)$ which involve generalized forces corresponding to external flow, cavity flow and boundary-layer turbulence. The generalized forces for cavity and external aerodynamics due to panel motion are described in detail in Ref. 4, while the generalized random forces from boundary-layer turbulence are given in Refs. 5 and 11. By assuming piston theory aerodynamics for the external supersonic flow and the shallow cavity approximation, the integral-differential equations reduce to a system of nonlinear differential equations which are solved numerically by a Monte Carlo technique.

The computation of generalized random forces as described in Ref. 11 could be time and cost consuming. To reduce computation time and improve accuracy, Fast Fourier Transform (FFT) techniques can be utilized.[12] Furthermore, when the simulated generalized random forces are ergodic, the ensemble averages can be replaced by temporal averages thereby reducing computation time.

The purpose of using random process theory in panel response analysis is to be able to judge the survivability of the panel under random excitation such as boundary-layer turbulence or jet noise. An elastic panel responding to random excitation acts as a "filter" passing frequencies in the vicinity of the natural frequencies of the panel. For a linear response this is evidenced by sharp peaks in the response spectrum at each natural frequency of the panel. However, when the response is nonlinear, resonance does not occur in the same manner as for linear response. Here the response amplitudes are limited and response frequency is a function of amplitude.[5] Furthermore, when fluid/solid interactions are included and a flutter ondition is reached, the response spectrum exhibits a distinct peak at the flutter frequency. Even though a considerable amount of work has been done on nonlinear panel response and flutter, it is not clear how this "nonlinear filtering" phenomenon affects statistics of panel response with regard to probability density function, peak distribution, threshold crossing, and spectral density.

The simulated generalized random force is gaussian by virtue of central limit theorem and for a linear system the distribution of response amplitude is also gaussian. However, for nonlinear system, the response is non-gaussian and no simple analytical technique is available to determine response probability structure. For this purpose numerical procedures need to be developed to produce histograms for probability density function.

Although design of panels to random inputs might be customarily concerned with the largest values of response, distribution of all responses becomes important when the question of fatigue arises. For this purpose the statistics of threshold crossing and peak distribution of panel response are required. To obtain threshold crossing, information from joint distribution of response processes w and $\dot{w}$ is needed. Similarly, peak distribution is obtained as soon as the joint distribution of w, $\dot{w}$, and $\ddot{w}$ is known. For nonlinear response analysis, this information is not available in a closed form. Thus, numerical techniques were developed to obtain response crossing at a specified threshold level and distribution of maximum and minimum peaks.

To obtain spectral density of panel response process, Fast Fourier Transform techniques were utilized. The finite Fourier transform of $w(t_n)$ at discrete frequencies ω_k can be written as

$$W(\omega_k) = \frac{W(\omega_k, T)}{\Delta t} = \sum_{n=0}^{N-1} w(t_n) \exp[-\mathbf{i} 2\pi k n/N], \qquad k = 1,2,\ldots,N \tag{2}$$

in which T is period and $t_n = n\Delta t$ with Δt being the time interval. Then, the numerical estimate of response spectral density at FFT discrete frequencies is[12]

$$S_w(\omega_k) = (2/N\Delta t)|W(\omega_k)|^2 \tag{3}$$

3. Boundary-Layer Turbulence

Most of the turbulent boundary-layer pressure data have been digested into a power spectral density form. A considerable amount of work, both theoretical and experimental, has been carried out on this subject with regard to panel response, panel flutter, and noise transmission.[4–7] For the purpose of this study, the semiempirical forms of cross spectra corresponding to subsonic flow given in Ref. 6 and to supersonic flow given in Ref. 7 were used for numerical computations. For homogeneous turbulence, the cross spectra can be approximated by

$$S(\xi,\eta,\omega) = S(\omega)|R(\xi,0,\omega)||R(0,\eta,\omega)|e^{-i\omega\xi/u_c} \quad 0 \leqq \omega < \infty \tag{4}$$

in which $R(\xi,\eta,\omega)$ is the correlation coefficient and $S(\omega)$ is spectrum.

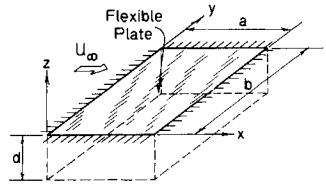

Fig. 2 Problem geometry.

For subsonic flow with an attached boundary layer, the empirical representations suggested in Ref. 6 are

$$S(\omega) = \frac{q^2\zeta}{u_\infty}\{3.7e^{-2\bar{\omega}} + 0.8e^{-0.47\bar{\omega}} - 3.4e^{-8\bar{\omega}}\} \times 10^{-5} \quad (5)$$

$$R(\xi, 0, \omega) = e^{-0.1\omega|\xi|/u_c} \quad (6)$$

$$R(0, \eta, \omega) = e^{-0.715\omega|\eta|/u_c} \quad (7)$$

where $\bar{\omega} = \omega\zeta/u_\infty$ and the convection speed u_c is assumed to be independent of frequency. At $u_\infty = 800$ fps, $\zeta = 0.157$, $u_c = 0.65u_\infty$.

For supersonic flow the proposed empirical formulas in Ref. 7 are

$$S(\omega) = \frac{q^2\zeta^*}{u_\infty}\{4.4e^{-0.0578\bar{\omega}} + 7.5e^{-0.243\bar{\omega}} - 9.3e^{-1.12\bar{\omega}} - 2.5e^{-11.57\bar{\omega}}\} \times 10^{-2} \quad (8)$$

$$R(\xi, 0, \omega) = e^{-|\xi|/\alpha_1\zeta^*} \quad (9)$$

$$R(0, \eta, \omega) = e^{-|\eta|/\alpha_2\zeta^*} \quad (10)$$

where $\bar{\omega} = \omega\zeta^*/u_\infty$. At $M = 2$ and $u_\infty = 1990$ fps, $\zeta^* = 0.91$ in., $\alpha_1 = 1.22$, $\alpha_2 = 0.26$, $u_c = 0.75u_\infty$.

In the panel response study when simulation of random processes is essential, it is necessary to take Fourier transform of Eq. (4) with respect to ξ and η. Then, the one sided wave number and frequency spectrums for subsonic and supersonic flows are, respectively

$$S(k_1, k_2, \omega) = S(\omega)\frac{(\omega/u_c)^2}{\pi^2\{(0.1\omega/u_c)^2 + (\omega/u_c + k_1)^2\}\{(0.715\omega/u_c)^2 + k_2^2\}} \quad (11)$$

$$S(k_1, k_2, \omega) = S(\omega)\left[\frac{1/\alpha_1\zeta^*}{(1/\alpha_1\zeta^*)^2 + (\omega/u_c + k_1)^2}\right]\left[\frac{1/\alpha_2\zeta^*}{(1/\alpha_2\zeta^*)^2 + k_2^2}\right]\frac{1}{\pi^2} \quad (12)$$

4. Numerical Results

General Nature

As pointed out in Refs. 1–3, panel response to turbulent boundary-layer excitation can be considered independent of initial conditions, i.e., displacement and velocity. The response may be expressed functionally as

$$w/h = w/h(\xi, \eta, \tau, a/b, M, \mu, \lambda, \mu^c, \lambda^c, \sigma) \quad (13)$$

in which σ = nondimensional rms pressure of boundary-layer pressure fluctuations, $\sigma = \alpha a^4\rho_\infty u_\infty^2/2hD$, where α is a parameter determined experimentally which can be taken equal to 0.0056 for subsonic flow and to 0.005 for supersonic flow.[14,15] In this paper we considered $a = 10$ in., $b = 20$ in., $h = 0.03$ in. for supersonic flow calculations and $h = 0.02$ in. for subsonic flow calculations, $\rho_m = 0.1$ lb/in.^{3}, $\nu = 0.3$, $E = 1 \times 10^7$ psi, $M = 0.8$ and $u_\infty = 800$ fps for subsonic flow, $M = 2.0$ and $u_\infty = 1990$ fps for supersonic flow. Response was computed for $\mu/M = 0.0275$ at $\xi = 0.75$ and $\eta = 0.5$ for supersonic flow, and $u/M = 0.14$ at $\xi = 0.5$, $\eta = 0.5$ for subsonic flow. The results were obtained for several values of parameters λ and σ for various combinations of in-plane loading, static pressure differential and cavity pressure. Response calculations were performed using one mode in the spanwise direction and six modes in the streamwise direction.

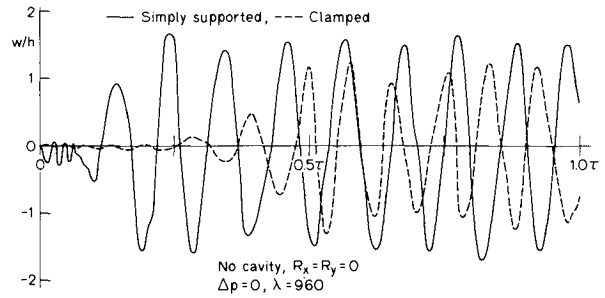

Fig. 3 Time history of nonlinear panel response.

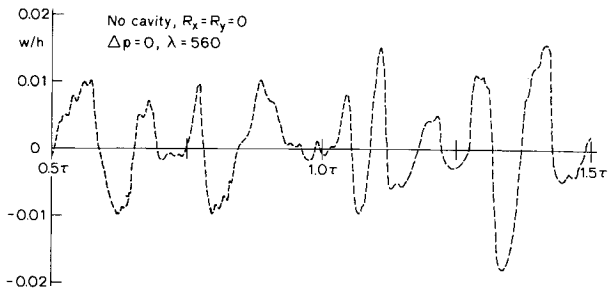

Fig. 4 Time history of linear panel response.

Linear–Nonlinear Response and Cavity Effect

In Fig. 2 problem geometry for deflection response calculations is shown. The panel is either simply supported on all four edges or clamped on all four edges. Utilizing Monte Carlo technique, time response histories of simply supported and clamped panels were obtained. The time histories shown in Fig. 3 correspond to nonlinear panel response and exhibit narrow band random process characteristics with apparent vibration frequency at the flutter frequency of the panel. In Fig. 4 time history of linear response is shown for a clamped panel and supersonic flow. As can be observed from this figure, linear response is a wide band random process. This is due to the fact that several modes are now excited by the wide band boundary-layer pressure field. The rms response is plotted in Fig. 5 against λ for supersonic flow for simply supported and clamped panels with and without cavity effect. These results indicate that for a panel with aspect ratio $a/b = 0.5$, response becomes nonlinear for $\lambda > 460$, simply supported panel no cavity, $\lambda > 430$, simply supported panel with cavity; $\lambda > 600$ clamped panel no cavity, $\lambda > 550$, clamped panel with cavity. These values were obtained based upon the upper limit of the linear portion of the curves presented in Fig. 5. Thus, for λ values larger than the ones indicated, a nonlinear type analysis is necessary.

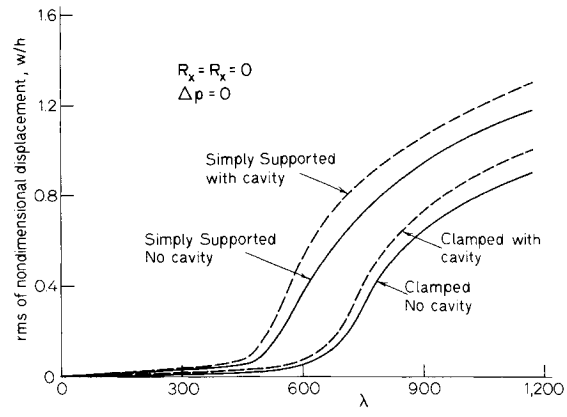

Fig. 5 The rms response under supersonic flow.

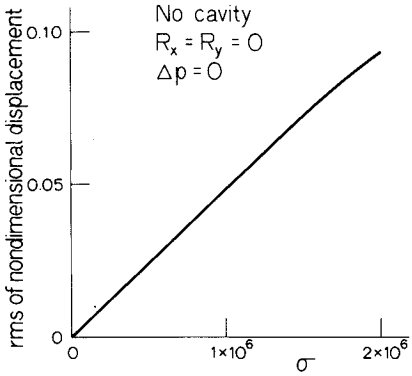

Fig. 6 The rms response under subsonic flow.

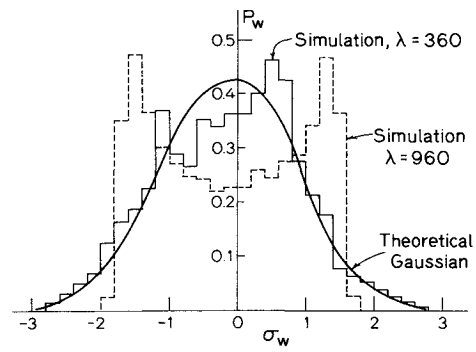

Fig. 9 Probability density function of response for supersonic flow.

The rms response for subsonic flow and clamped support conditions is plotted in Fig. 6 against σ. It can be observed from these results that panel response to subsonic flow would become nonlinear for very large values of parameter σ. The effect of external aerodynamic pressure and cavity pressure is neglected in this case. However, if cavity pressure is included, panel response under subsonic flow would be reduced.[5]

Panel under In-Plane Loads

The in-plane loads usually arise from a temperature differential between plate and boundary support. The range of values chosen for in-plane loading includes loads below and above buckling. The classical Euler buckling load for a simply supported plate with aspect ratio $a/b = 0.5$ and equal compressive loading on all four edges is $R_x = R_y = -1.25\pi^2$, where R_x and R_y are nondimensional in-plane loads, i.e.,

$$R_x = N_x a^2/D, \quad R_y = N_y a^2/D$$

with N_x and N_y being the in-plane stress resultants externally applied. Buckling load for the same panel but with clamped edge conditions is approximately equal to $R_x = R_y = -3.95\pi^2$ (Ref. 13). Results were also obtained for the cases when in-plane loads are applied in tension.

The rms of clamped and simply supported panels is given in Fig. 7 for several values of R_x. As can be observed from these results, tensile in-plane loads tend to stabilize panel response while compressive loads tend to increase panel response. The compressive loads which are far below the critical buckling load of the panel have only small effect on panel response. However, when compressive in-plane loads exceed critical buckling load, panel response is modified significantly and panel nonlinearities become more important for this case. Furthermore, with increasing value of R_x in the postbuckling region the response amplitudes increase in nonlinear fashion (Fig. 7). This is due to nonlinear terms included in equations of motion (1–3).

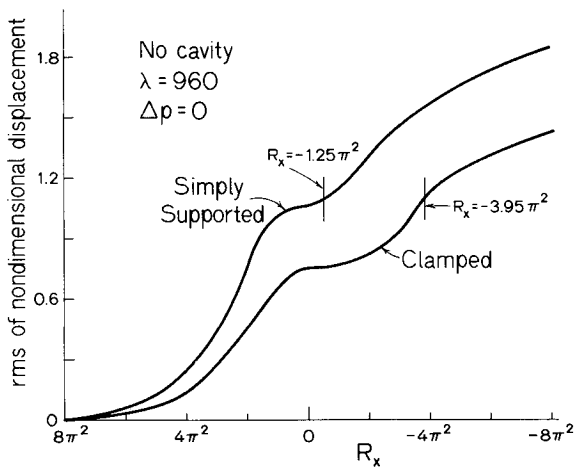

Fig. 7 The rms response with in-plane loading.

Effect of Static Pressure Differential

A panel under the influence of uniform static pressure undergoes a static deformation. Time histories of a clamped panel in supersonic flow are shown in Fig. 8 for two values of static pressure differential Δp. The mean response and rms response values are also indicated in this figure. As can be seen from these results, dynamic panel response stabilizes at a static deflection position with increasing static pressure differential. Similar response trends were observed for a simply supported panel.

Probability Structure of Panel Response

From panel response time histories, histograms of probability density function were computed vs standard deviation σ_w of nondimensional panel response. In Fig. 9, histograms of probability density function for a clamped panel and supersonic

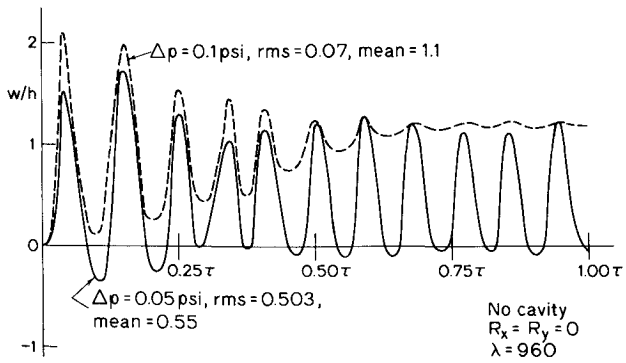

Fig. 8 Time history of panel response with static pressure.

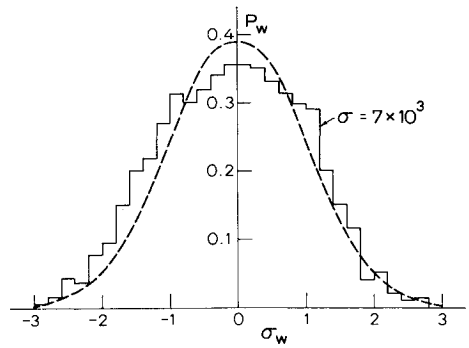

Fig. 10 Probability density function of response for subsonic flow.

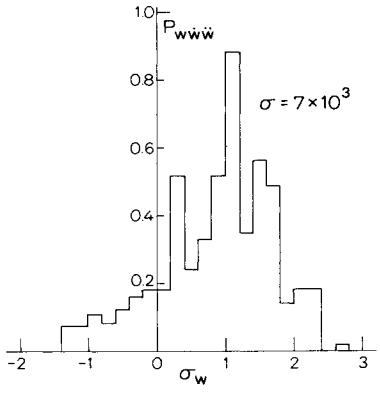

Fig. 11 Probability density function of response peak distribution for subsonic case.

flow are shown for two values of parameter λ, i.e., corresponding to linear and nonlinear response. With decreasing λ, response amplitude distribution tends towards a gaussian form, while nonlinear response exhibits nongaussian distribution. Similar results are presented in Fig. 10 but for subsonic flow and linear panel response. Theoretical distribution curves corresponding to linear response are also presented in these figures. Histograms of probability density function for a simply supported panel show similar distribution trends.

Peak Distribution

The probability density of the peaks for a clamped panel and subsonic flow is given in Fig. 11. Similar results are presented in Fig. 12 for supersonic flow. In Fig. 13, peak distributions are given for the same panel under supersonic flow for the cases with in-plane loading, static pressure differential and cavity effect. These results indicate that for nonlinear response, peaks are clustered at a specific threshold level σ_w while linear response shows a wider peak distribution.

Threshold Crossing

Deflection response crossing rate at various threshold levels for σ_w is presented in Fig. 14 for a clamped panel under subsonic boundary-layer flow. Threshold crossing for supersonic flow is given in Fig. 15 for simply supported and clamped panels.

Response Spectral Density

Nondimensional deflection response spectral densities were computed by applying FFT technique to response time history of the panel. For clamped panels, spectral densities are plotted against frequency parameter $\omega^* = \omega(D/\rho_m h a^4)^{-1/2}$ where ω is vibration frequency in rad/sec. Response spectral density for a clamped panel and subsonic flow is given in Fig. 16. Since deflection response was computed at the midspan for this case, only peaks corresponding to odd modes appear. Because turbulent boundary-layer pressure spectrum for subsonic flow

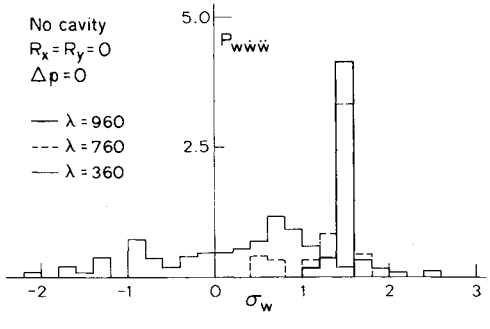

Fig. 12 Probability density function of response peak distribution for supersonic case.

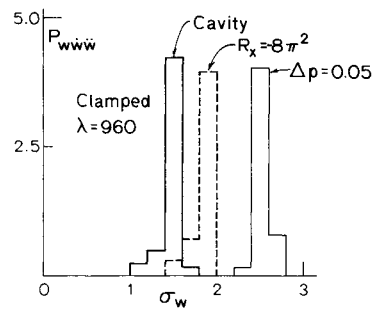

Fig. 13 Probability density function of response peak distribution with cavity, in-plane loading and static pressure.

has a peak near $\omega^* = 250$, higher modes are amplified more than the lower modes. In Figs. 17 and 18, response spectral densities for the same panel but supersonic flow at $\xi = 0.75$ are given for several values of parameter λ. These results indicate a gradual merge of first and second mode peaks into one peak as the value of parameter λ approaches the flutter condition. Response spectral density for a simply supported panel and supersonic flow is plotted in Fig. 19 but against frequency ω instead of ω^* as used for clamped panel.

5. Remarks on Simulation and Computation

The method used in this paper provides an efficient tool in studying intensities and statistical properties of flexible elastic

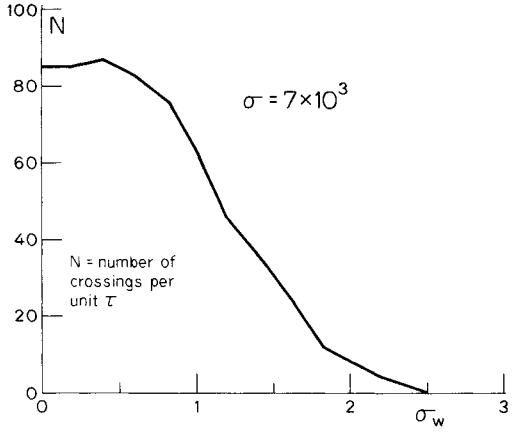

Fig. 14 Response threshold crossing for subsonic flow.

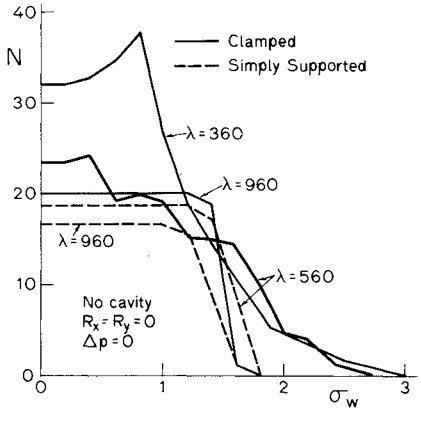

Fig. 15 Response threshold crossing for supersonic flow.

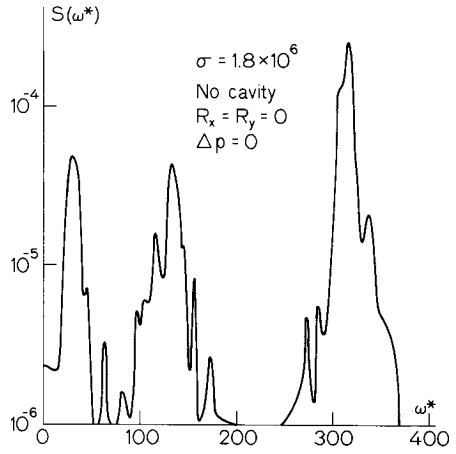

Fig. 16 Response spectral density for subsonic flow.

panels to subsonic and supersonic boundary-layer turbulence. This method is not limited only to boundary-layer turbulence excitation. It can be extended to accommodate any multidimensional or multivariate random excitation.

The response calculations were obtained over time interval 3.4τ. The computer time for a typical run on IBM 360/91 was about 50 sec. This includes simulation of boundary-layer turbulence, numerical integration of equations of motion, temporal averaging to obtain rms values, calculations of probability density, peak distribution, threshold crossing and response spectral density.

6. Conclusions

In this paper criteria for nonlinear response of clamped and simply supported panels were established. The dynamic response amplitudes of fixed panels were found to be about 33% lower than those of simply supported panels under identical flow conditions. Maximum response amplitudes were observed on the order of 1.6 times the over-all rms value for nonlinear response, and on the order of 3.0 times the over-all rms value for linear response. When cavity préssure or compressive in-plane loading was included, panel response amplitudes were increased under supersonic flow conditions. The effect of static pressure differential was to decrease vibration amplitude and to stabilize panel response to a fixed static position.

It was observed that the probability structure of linear panel response is gaussian while nonlinear response is nongaussian exhibiting a bimodal type distribution. This is due to the fact that the rate of response increase is large when panel goes through neutral equilibrium position and no stretching of the midplane surface occurs. However, when deflections reach nonlinear range, midplane stretching occurs slowing down the rate of deflection. Thus, probability density function is at a maximum when σ_w reaches response peaks and then drops sharply to zero since the peaks are concentrated in a narrow band as can be observed from peak distribution results.

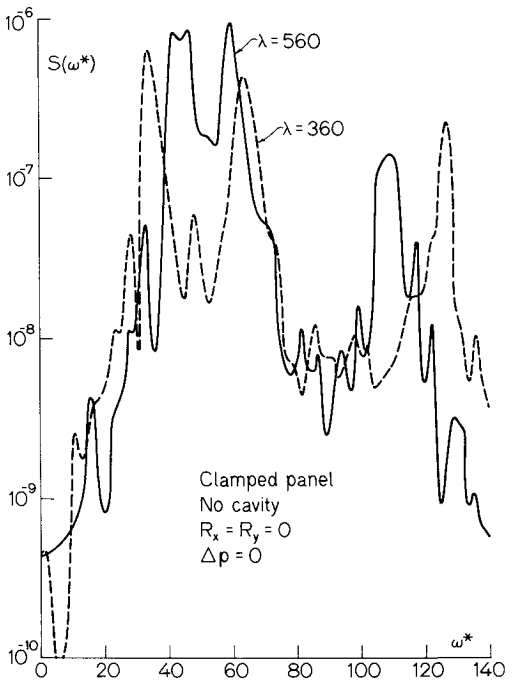

Fig. 17 Linear response spectral density for supersonic flow and clamped panel.

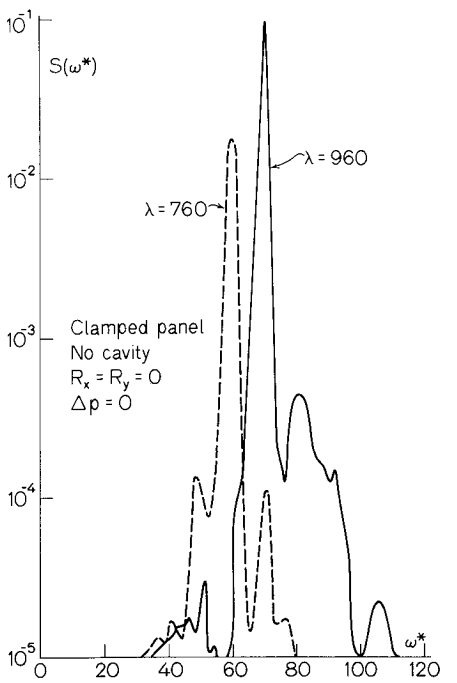

Fig. 18 Nonlinear response spectral density for supersonic flow and clamped panel.

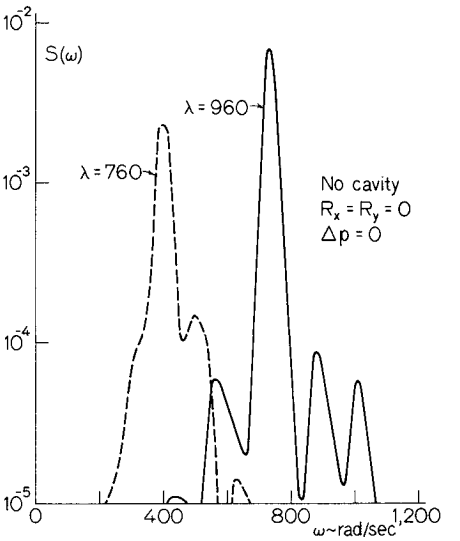

Fig. 19 Nonlinear response spectral density for supersonic flow and simply supported panel.

Threshold crossing rate of clamped panels was observed to be about 3 crossings/unit τ higher than for simply supported panels. This would indicate a shorter fatigue life for clamped panels at a given stress level. The effect of in-plane loads, static pressure differential and cavity pressure on peak distribution and threshold crossing was to extend distribution and crossing regions to higher levels of σ_w. It was observed that the linear response showed a wider range of peak distribution and higher crossing rates than nonlinear response.

Spectral density corresponding to linear response exhibited peaks at the natural frequencies of the panel. However, when response amplitudes reached nonlinear panel flutter region, only one distinct peak at the flutter frequency occurred. This peak occurred at a frequency slightly lower than the second mode natural frequency of the panel. The input spectrum corresponding to boundary-layer turbulence is wide band random process as can be observed from Fig. 1. Thus, many vibration modes could be excited. However, when panel response reaches flutter condition, the response is dominated by the external aerodynamic pressure with boundary-layer turbulence having only a small effect. This phenomenon is clearly observed from response spectral densities (Figs. 16–19) where a gradual excursion into flutter region is shown.

References

[1] Dowell, E. H., "Nonlinear Oscillations of a Fluttering Plate I," *AIAA Journal,* Vol. 4, No. 7, July 1966, pp. 1267–1275.

[2] Dowell, E. H., "Nonlinear Oscillations of a Fluttering Plate II," *AIAA Journal,* Vol. 5, No. 10, Oct. 1967, pp. 1856–1862.

[3] Dowell, E. H., "Transmission of Noise from a Turbulent Boundary Layer through a Flexible Plate into a Closed Cavity," *Journal of the Acoustical Society of America,* Vol. 46, No. 1, Pt. 2, 1969, pp. 238–252.

[4] Dowell, E. H., "Panel Flutter: A Review of Aeroelastic Stability of Plates and Shells," *AIAA Journal,* Vol. 8, No. 3, March 1970, pp. 385–399.

[5] Vaicaitis, R., Jan, C. M., and Shinozuka, M., "Nonlinear Panel Response from a Turbulent Boundary Layer," *AIAA Journal,* Vol. 10, No. 7, July 1972, pp. 895–899.

[6] Bull, M. K., "Wall-Pressure Fluctuation Associated with Subsonic Turbulent Boundary Layer Flow," *Journal of Fluid Mechanics,* Vol. 28, Pt. 4, 1967, pp. 719–754.

[7] Maestrello, L., "Radiation from a Panel Response to a Supersonic Turbulent Boundary Layer," *Journal of Sound and Vibration,* Vol. 10, Feb. 1969, pp. 261–275.

[8] Shinozuka, M., "Simulation of Multivariate and Multidimensional Random Processes," *Journal of the Acoustical Society of America,* Vol. 49, No. 1, Pt. 2, 1971, pp. 357–367.

[9] Shinozuka, M. and Jan, C. M., "Digital Simulation of Random Processes and Its Applications," *Journal of Sound and Vibration,* Vol. 25, No. 1, 1972, pp. 111–128.

[10] Ventres, C. S., "Nonlinear Flutter of Clamped Plates," Ph.D. thesis, Oct. 1969, Aerospace and Mechanical Sciences Dept., Princeton Univ., Princeton, N.J.

[11] Vaicaitis, R., "Generalized Random Forces for Rectangular Panels," *AIAA Journal,* Vol. 11, No. 7, July 1973, pp. 984–988.

[12] Bendat, J. S. and Piersol, A. C., *Random Data: Analysis and Measurement Procedures,* Wiley-Interscience, New York, 1971.

[13] Masatsugu, K. et al., *Handbook of Elastic Stability,* N69-34698, 1969, NASA.

[14] Lin, Y. K., *Probabilistic Theory of Structural Dynamics,* McGraw-Hill, New York, 1967, pp. 218–219.

[15] Bull, M. K., Wilby, J. F., and Blackman, D. R., "Wall Pressure Fluctuation in Boundary Layer Flow and Response of Simple Structure to Random Pressure Fields," A.A.S.U. Rept. 243, 1963, Univ. of Southampton, Southampton, England, pp. 1–28.